Rat electrophysiological signal analysis

Internship report

Samuel Ortion[1]

Supervisor: Nicolas Fourcaud-Trocmé

Lyon Neuroscience Research Center

[1] L3 Licence double Informatique - Sciences de la vie
University of Évry – Paris-Saclay University

From May 15th to July 7th 2023

Abstract

In previous experiments, rats were trained to perform an odor discrimination task.

Phase reset is known to be a common phenomenon in brain rhythms after a sensory stimulus. We investigated phase reset of brain rhythms, as well as respiratory signal. We found a phase reset in sniffing rhythms. The other signals did not show a conclusive phase reset, on the time references we used.

We also searched for amplitude modulation of brain rhythms through learning, using time-frequency maps. We reproduced the result of β frequency up modulation during learning and found some other interesting modulations in different time-frequency windows.

Finally, we investigated connectivity between recorded brain regions. We studied more specifically the connectivity of hippocampal θ rhythm and respiratory / olfactory bulb lower θ rhythm, to study the evolution of brain networks during odor learning.

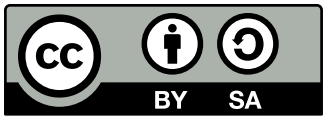

Contents

List of Figures

List of Tables

Abbreviations

AP Anterior Piriform cortex 1–4, 6, 8

Cereb Cerebellum 1, 2

Hipp Hippocampus 1–3, 6, 8

LFP Local Field Potential ii, 2, 3, 5, 11

OB Olfactory Bulb 1–3, 6–9, 11

OT Olfactory Tubercle 1–3, 6, 8

PP Posterior Piriform cortex 1–3, 6, 8, 9

Respi Respiration 3

Stri Striatum 1–3, 6, 8

TF-map Time-Frequency map 4, 6

wPLI weighted Phase Lag Index 6, 8–11

1 Introduction

Olfaction is undoubtedly an important sense for rodents. Indeed, it has a strong influence on their behaviour, as it is involved in finding food as well as social relationships. Odor sampling depends on respiratory rhythms: odorant molecules are driven onto the olfactive epithelium at each inspiration / expiration cycle. It has been shown that respiration modulates olfactory neurons activity [3], as well as non-olfactory neurons [7].

LFP and brain rhythms In the present work, we used intra-cranial recordings of local field potentials (LFP). LFP are the result of the sum of the activity of neurons in the vicinity of a recording electrode, implanted inside the brain tissue. LFP recordings show often rhythmic activity or oscillations (see figure 3)

Oscillations of LFP are an important feature of the brain. Oscillations appear to be a fundamental mechanism for the coordination of neuronal activity, as well as communication between brain regions, for instance [4].

Olfactory system is characterized by numerous LFP oscillations. These oscillations are either slow, related to the respiratory rhythm (especially in the Olfactory Bulb (OB)), or faster, such as β and γ rhythms which are rather related to perception and memory.

The aim of this internship was to study the evolution of such brain rhythms during the learning of an olfactory discrimination task in rats, by analyzing the phase, amplitude and synchronization of these oscillations between distant brain areas.

2 Methods and Results

The analyses were performed on data acquired by Lefèvre et al. [8] in 2014 at CRNL.

2.1 Experiments

The experiments are described in [5, 8]. Briefly: thirteen rats were implanted with stainless steel LFP recording electrodes soldered to copper wire in Olfactory Bulb (OB), Anterior Piriform cortex (AP), Posterior Piriform cortex (PP), Olfactory Tubercle (OT), dorsal Striatum (Stri), dorsal CA1 of the Hippocampus (Hipp), and Cerebellum (Cereb). For reference, a diagram of the location of the recorded brain structures is shown in figure 1.

LFP signals were transmitted remotely to the acquisition machine. Rats were placed in a whole body plethysmograph allowing to record respiratory rhythms (as described in [6]).

A central odor port with capacitive sensor allowing nose poke detection delivered one of a pair of odor. Two lateral reward ports were able to deliver water. The right or left

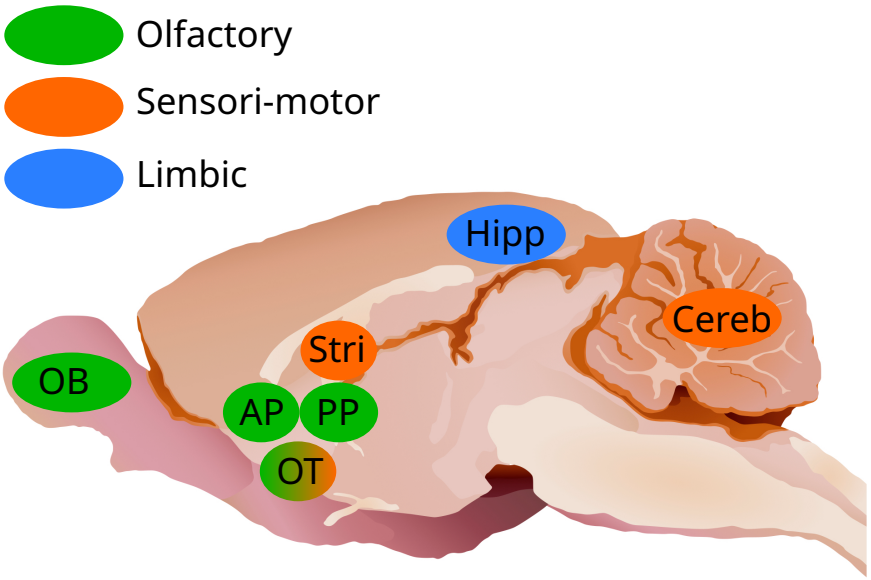

Figure 1: Localization of rat brain structures where LFP probes were implanted. Local Field Potential (LFP) were recorded in Olfactory Bulb (OB), Anterior Piriform cortex (AP), Posterior Piriform cortex (PP), Olfactory Tubercle (OT), Striatum (Stri), dorsal Hippocampus (Hipp) (CA1 cells) and Cerebellum (Cereb).

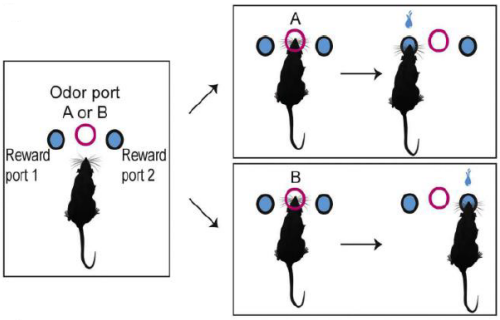

(a) Odorant pair discrimination

(b) Whole body plethysmograph

Figure 2: Experimental setup of the discrimination training. **(a)** Rats were trained to discriminate a pair of odorants. A trial was initiated by rat nose poke on odor port (pink circle). The rat had 6 s to make a choice. If the rat chose the correct port, it was rewarded with water. **(b)** The experiment took place in a whole body plethysmograph allowing to record respiratory rhythms. (source: [8])

reward port were associated with the odor. The rat had only 6 s to chose the correct port. Whenever the rat chose the incorrect port, no water reward was delivered (see figure 2a).

Several experiment phases with distinct odor pairs were performed. Phases P1, P2 and P3 were associated with distinct odor pairs. In these phases, several test days occurred, namely S1, S2, ..., S_n, LC0 LC1, ..., LC_n, where LC1 is the first test day where rat obtained more than 80% of success.

The experiment took place in a whole body plethysmograph allowing to record respiratory rhythms (see figure 2b).

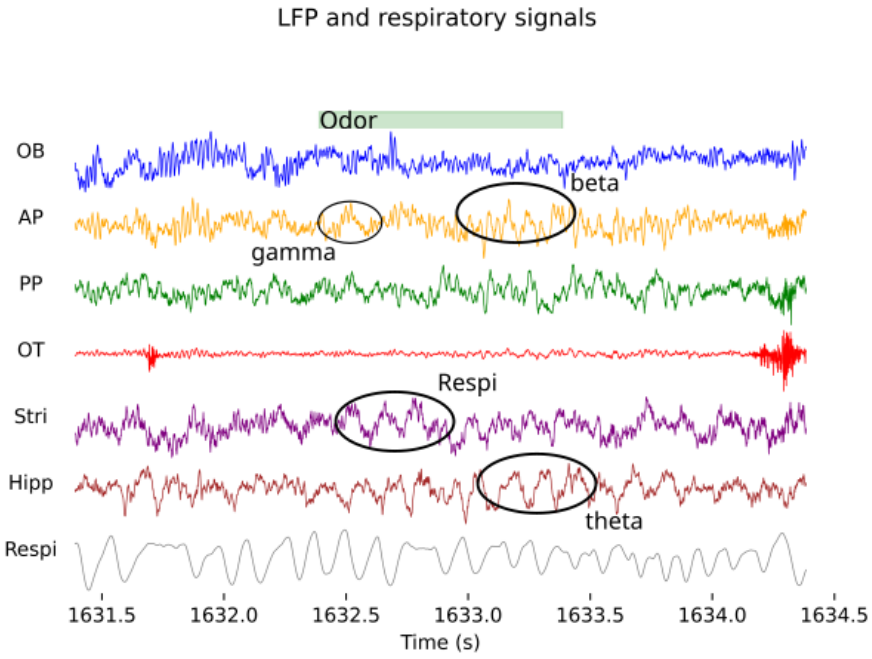

Figure 3: LFP and respiration signals extract, available from Lefèvre's dataset [5, 8]. Rats Local Field Potential (LFP) were recorded in Olfactory Bulb (OB), Anterior Piriform cortex (AP), Posterior Piriform cortex (PP), Olfactory Tubercle (OT), Striatum (Stri), and dorsal Hippocampus (Hipp) (CA1). Respiration (Respi) signal was recorded with a plethysmograph. Stereotypical rhythms (theta, beta, Respi, and gamma) are annotated on the figure.

2.2 Analysis

All subsequent data analyses have been performed using home-made Python scripts with the help of Python libraries such as numpy, pandas, scipy, xarray, and others. Basic SnakeMake analysis pipelines were written to automate the analyses, and launch them easily on the Slurm cluster [9].

2.2.1 Phase reset

In order to detect if the animals synchronized their respiration and slow brain rhythms at the starting of the trial, a phase reset analysis was conducted.

Signals were band pass filtered in 5-15 Hz (slow rhythms were privileged, as higher frequencies are unlikely to show up phase resets). Then, the phases of the signals were computed using Hilbert transform. Trial phases were aligned on the time of nose poke in a time window of 2 s on each side. An example of LFP signal phase around nose poke is shown in figure 4. The phase of each trial at a given time were stacked and a Rayleigh test was performed to detect phase synchronization. Then, the z-scores of the Rayleigh test p-values were computed.

A phase reset plot of Rayleigh test p-value Z-scores for respiratory signal is presented figure 5. A phase reset of respiratory signals occurs for rats entering the odor port.

No phase reset in θ-hippocampal LFP signal could be identified. This may be due to the small random latency between detected nose poke and real release of the odor, which could lead to an asynchrony between brain rhythms associated with the treatment of the odorant signal and decision making. It may also be caused by inherent variability in latency for θ rhythm induction in the rat brain.

2.2.2 Time-frequency maps and amplitude modulation

It has already been shown that β oscillations in the Anterior Piriform cortex (AP) were up modulated throughout the learning of this very task [5]. We wanted to look at the modulation of other brain rhythms.

In order to study the modulation of brain rhythms amplitude during learning, we measured the intensity of the signal in specific time-frequency windows.

Time-frequency power maps were computed using standard Morlet wavelet transform, with $\sigma = 5\pi$ [5]. Time Frequency maps were computed for each trial's whole time range.

TF-maps averaged across trials were computed and showed some interesting frequency modulation pattern, when trial variability was smoothed. One of such an averaged Time-Frequency map (TF-map) is shown in figure 6. In this figure, a region of interest is outlined in γ frequency band. Such regions, noticed in averaged TF-map were used to compute local amplitude modulation across sessions and within a session in different time-frequency windows. The median in a reference zone in the same frequency band but before the odor port entry (-1--0.6 s), was used to normalize the amplitude modulation. Measures were computed on a trial by trial basis. The modulation in amplitude of the signal in β band (12 - 30 Hz) was measured as the 3$^{\text{rd}}$ quartile between -0.4 and 0.2 s around odor port exit.

A modulation in amplitude of the LFP signal in β band around odor port exit appears correlated to rat performance, in different brain regions, such as olfactory bulb

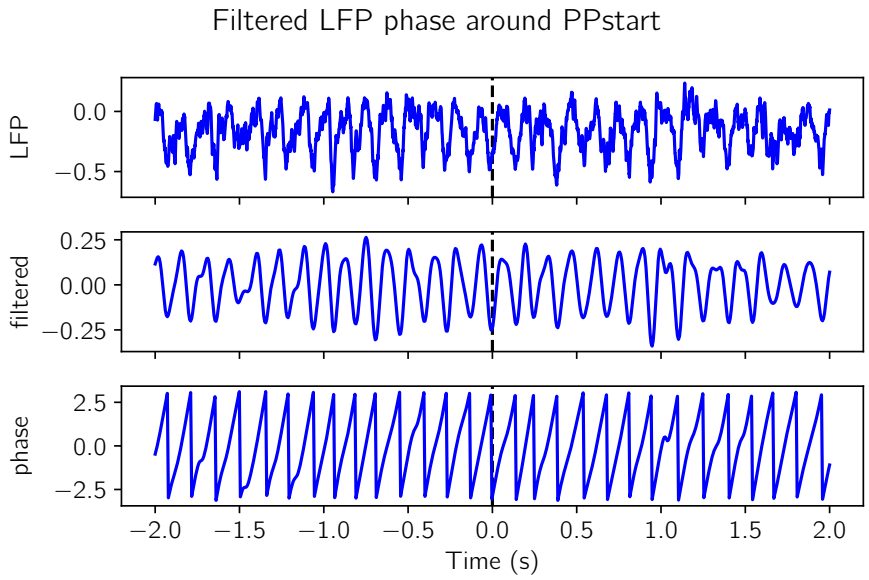

Figure 4: Phase of LFP signal after filtering in 5-15 Hz band, from hippocampal LFP of rat `Rtbsi11`. Phase of signal is computed using Hilbert transform. A time window of 2 seconds on each side of the nose poke is shown.

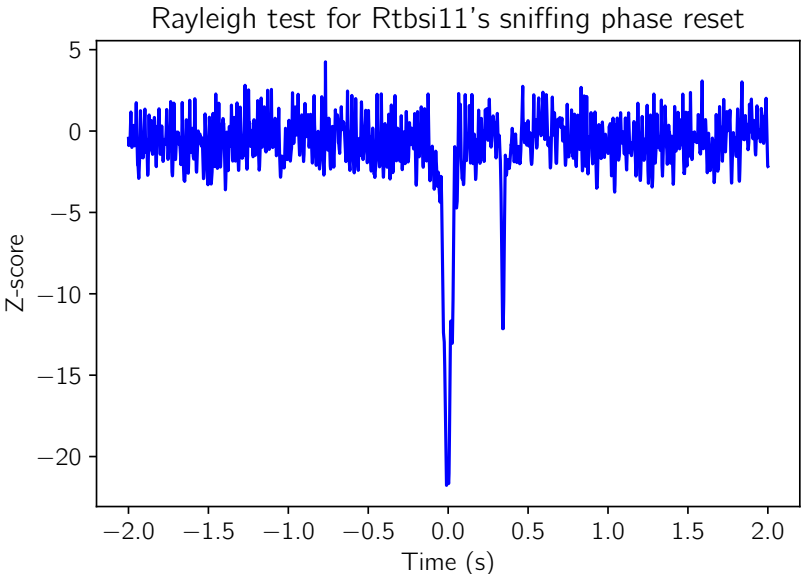

Figure 5: Respiratory signal phase reset for rat `Rtbsi11`. Signal were filtered in 5-15 Hz band. Hilbert transform was used to compute the phase of the signal. Phases of signal for each trial were aligned to entry in odor port in 2 s windows on each side around this timestamp. Rayleigh test was performed on phase distributions at each time step. Then, the Z-scores of these p-values were computed.

(see figure 7). This modulation can be seen in different other recorded brain regions, such as Olfactory Tubercle (OT), Striatum (Stri) and Posterior Piriform cortex (PP). As shown by Fourcaud-Trocmé et al. [5], this modulation is also present in AP. The increase in β-amplitude appears in the 25 first sessions of a given phase, then tend to stabilize (figure 8).

Among other brain rhythms studied, the θ rhythm showed up an interesting modulation pattern, as presented in figure 6B. In a manner similar to β amplitude measure, the 3$^{\text{rd}}$ quartile of signal intensity in -2 to -1 s around odor port exit in 7.5-10 Hz band (upper theta), and in -0.1 to 0.1 s in 6-7 Hz band (lower theta). The upper θ rhythm is up-modulated through learning, while the lower θ rhythm is down-modulated (figure 9).

2.2.3 Connectivity measures

A measure of phase synchronization between distant brain areas was used to decipher the evolution of brain connectivity through learning.

WPLI weighted Phase Lag Index (wPLI) is an indicator on signal connectivity, based on the phase difference between two signals.

This metrics was chosen as it tries to reduce the impact of volume conduction, which usually causes the two signals to share the exact same phase, even if there is no real neuronal connectivity between the two regions [2, 10]. Weighted Phase Lag Index (wPLI) ranges from 0 to 1, where 0 indicates no detected phase synchronization (or exact same phase, in case of volume conduction), and 1 indicates a constant phase difference between the two signals.

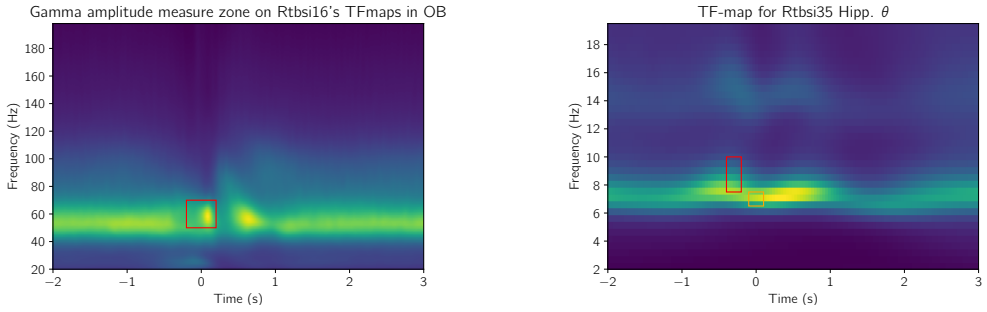

(a) **(b)**

Figure 6: Examples of TF-map, averaged across trials and aligned on odor release end. **(a)** In γ frequency band for rat `Rtbsi16` in OB. A region of interest is outlined in γ frequency band. **(b)** In θ frequency band for rat `Rtbsi35` in Hippocampus (Hipp), a TF-map showing a little "swirl" in frequency modulation. An harmonic of the modulated spot is also visible, at twice the frequency. A red and an orange square represent the time-frequency windows used to measure amplitude modulation of upper and lower θ respectively. Greenish color indicates higher power in the corresponding time-frequency bin.

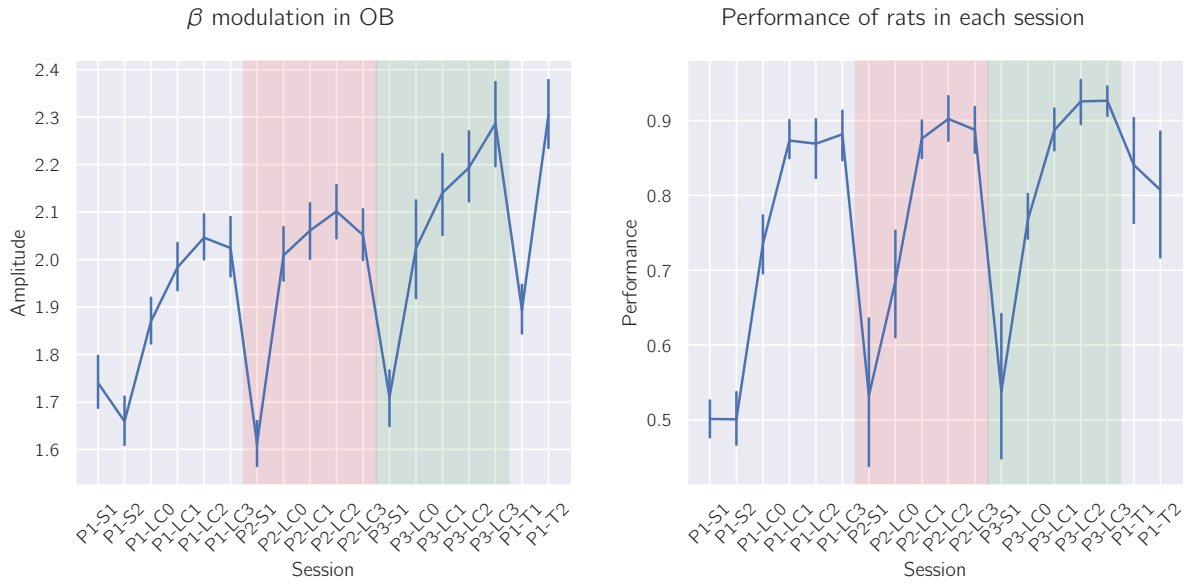

(a) β modulation in Olfactory Bulb (OB) **(b)** Rat performance

Figure 7: Amplitude modulation of β rhythm in olfactory bulb follows the same pattern as rat performance across sessions. **(a)** Amplitude modulation of β rhythm in olfactory bulb across sessions, measured with 3rd quartile of β amplitude in -400 ms up to 100 ms around odor port exit, in 12-30 Hz band. New odor pair is introduced at each change in phase (P1-P2-P3-P1), pair of odor periods are represented as color bands. **(b)** Rat performance across sessions, as number of correct trials over total number of trials. A trial is considered as correct whenever the rat headed first to the odor port that were associated with the odor presented, thus receiving the water reward. **(a)** & **(b)** Error bars corresponds to 95% confidence interval for the mean.

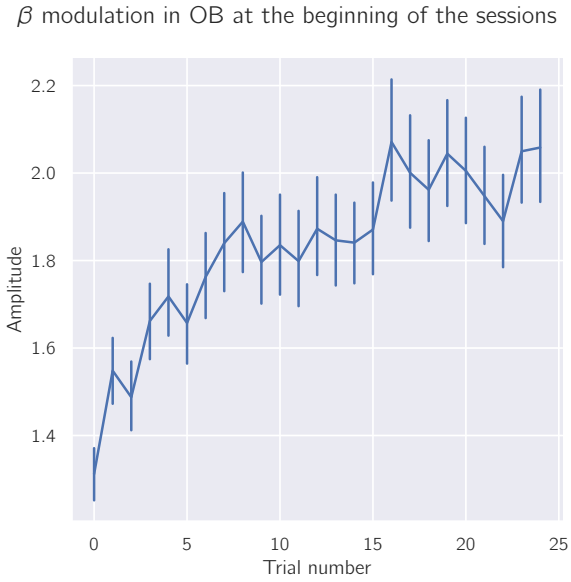

Figure 8: β increase in sessions in OB. Amplitude modulation of β rhythm in olfactory bulb inside sessions, measured on 3rd quartile of β amplitude in -400 ms up to 100 ms around odor port exit, in 12-30 Hz band. All sessions are mixed and the first 25 trials in a session are selected. The line is the average across rats of the average measure across sessions for each rat. Error bars represents 95% confidence interval for the mean.

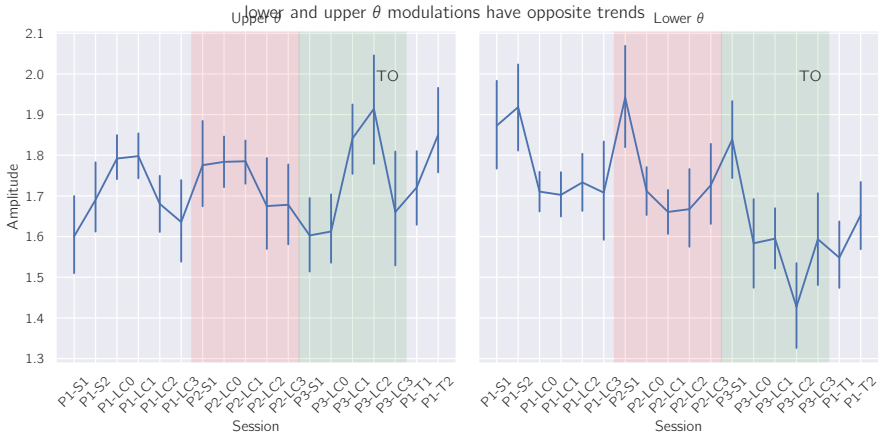

Figure 9: θ opposite modulations across sessions in Olfactory Tubercle (OT). Upper θ measured in -2 to -1 s around odor port exit in 7.5-10 Hz band (left panel), lower θ measured in -0.1 to 0.1 s in 6-7 Hz band (right panel). New odor pair is introduced at each change in phase (P1-P2-P3-P1), pair of odor periods are represented as color bands. Error bars corresponds to 95% confidence interval for the mean across rats.

WPLI was computed using the `spectral_connectivity` Python package. It was estimated frequency by frequency on precomputed wavelet spectra.

A time-frequency map of wPLI was computed for each session and for each pair of probes. One of such a map is presented in figure 10. On this map, there is a stronger connectivity between OB and PP probes in 12-15 Hz, close to the nose poke event.

On such a connectivity measures, available on whole time-frequency domain, a measure in a narrower zone (6-10 Hz, 0-500 ms) was computed using a method similar to the one used for TF-map amplitude modulation measures (figure 11 presents this modulation across sessions). The connectivity between region pairs seems to remain relatively stable across sessions, despite rat learning, at least in the time-frequency window considered.

On the other hand, a measure of wPLI was computed frequency by frequency, in order to observe the modulation of connectivity in different frequency bands. WPLI measure through frequency is presented for each pair of brain regions in session P1-S1 in figure 12. Between OB region and other regions such as AP, PP, Stri and OT, there is a strong wPLI peak in 6-9 Hz, in respiratory and θ frequency bands. We can see another strong wPLI peak (and a second peak which may correspond to a harmonic) between Hipp and AP, PP, Stri or OT. These observations lead to a model of neuronal network connectivity: respiratory rhythm, that originates from OB propagates to AP, PP, Stri and OT. Hippocampal θ rhythm, propagates to AP, PP, Stri and OT (figure 12).

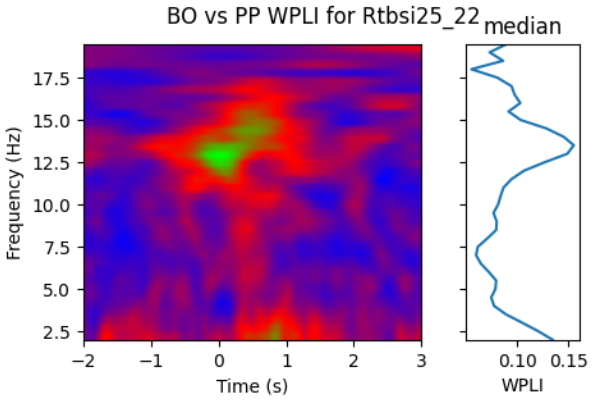

Figure 10: wPLI between Olfactory Bulb (OB) and Posterior Piriform cortex (PP) probes as time-frequency map for rat `Rtbsi25` in session P1-LC2. wPLI were computed for each frequency from standard Morlet wavelet spectra. The median wPLI across frequency is presented next to the corresponding TF-map. Blue color indicates low wPLI values, whereas red and green colors indicates higher wPLI values (i.e higher connectivity).

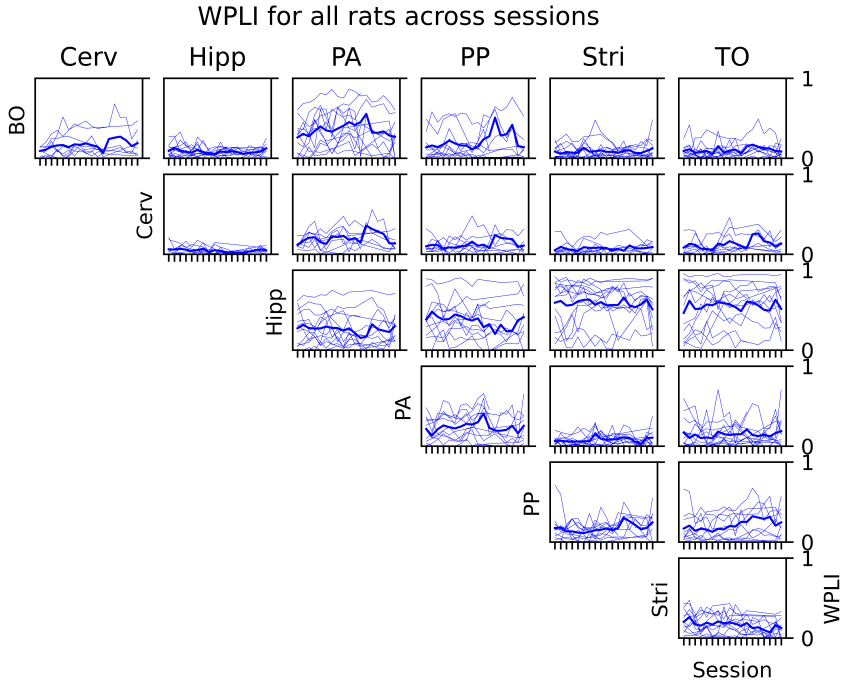

Figure 11: wPLI across sessions for all rats in a time-frequency region. wPLI is computed between each zone pairs, given by line and column. A measure of mean wPLI is computed in 6-10 Hz, 0-500 ms time-frequency region. The sessions presented are the same as in figure 7. Each lighter blue lines represents a rat. The bolder line is the average of all rats.

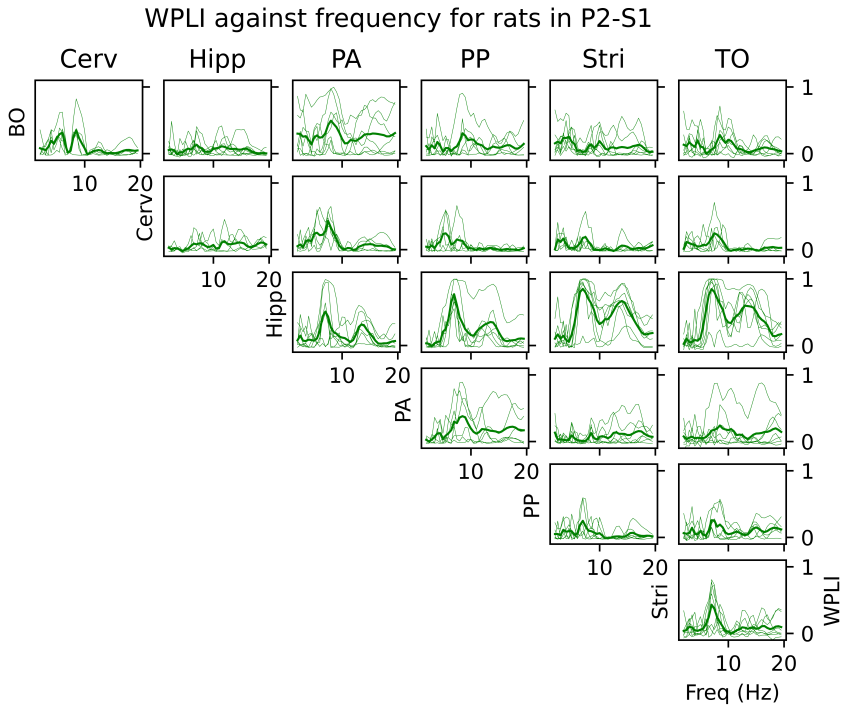

Figure 12: WPLI connectivity modulation in frequency, for rats in session P2-S1. WPLI is computed between each zone pairs, given by line and column, in whole time frequency domain from standard Morlet wavelet spectra. On wPLI matrix, a 25 ms time range after nose poke was selected and the median of wPLI was computed for each frequency, by 0.5 Hz step. Each lighter green lines represents a rat. The bolder line is the average of all rats.

3 Conclusions and Perspectives

The analyses of the previously collected data allowed to observe a phase reset of the respiratory rhythms at the entry in odor port. We could not show the same phase reset for LFP signal in hippocampal θ band, probably due to the variable latency between nose poke and odor release, or the variability in θ rhythm induction after sensory stimuli. We found a modulation in β LFP oscillations in several brain regions, such as OB following a similar pattern as rat performance across session and within session throughout rats' task learning. Finally, we could not observe a strong modulation in weighted Phase Lag Index (wPLI) connectivity between brain regions.

To go further, one could try to compute phase reset of LFP signal in hippocampal θ band using other reference timestamps, such as the time of the slower respiratory cycle occurring at the end of odor sampling, or at the exit of the odor port, for instances. A more precise analysis of connected neural networks could be explored, using graph theory backed technics [1], for instance.

During this internship, I learned the basics of neuroscience, and some of the techniques used to analyze LFP signals. This internship was the occasion to discover a bit of signal processing methods. I learned how to use Slurm on the lab computing cluster, as well as the basics of pipeline programming with SnakeMake too.

Throughout this two months, I had the opportunity to attend several presentations from CRNL researchers, allowing me to perceive a bit of the diversity of topics studied there.

References

[1] Dániel L. Barabási et al. *Neuroscience Needs Network Science*. May 11, 2023. DOI: 10.48550/arXiv.2305.06160. arXiv: 2305.06160 [q-bio]. URL: http://arxiv.org/abs/2305.06160 (visited on 06/11/2023). preprint.

[2] André M. Bastos and Jan-Mathijs Schoffelen. "A Tutorial Review of Functional Connectivity Analysis Methods and Their Interpretational Pitfalls." In: *Frontiers in Systems Neuroscience* 9 (2016). ISSN: 1662-5137. URL: https://www.frontiersin.org/articles/10.3389/fnsys.2015.00175 (visited on 06/16/2023).

[3] Nathalie Buonviso, Corine Amat, and Philippe Litaudon. "Respiratory Modulation of Olfactory Neurons in the Rodent Brain." In: *Chemical Senses* 31.2 (Feb. 1, 2006), pp. 145–154. ISSN: 0379-864X. DOI: 10.1093/chemse/bjj010. URL: https://doi.org/10.1093/chemse/bjj010 (visited on 06/14/2023).

[4] György Buzsáki. "Rhythms of the Brain." In: Oxford University Press, Oct. 26, 2006. ISBN: 978-0-19-530106-9. DOI: 10.1093/acprof:oso/9780195301069.001.0001. URL: https://academic.oup.com/book/11166 (visited on 01/12/2023).

[5] Nicolas Fourcaud-Trocmé et al. "High Beta Rhythm Amplitude in Olfactory Learning Signs a Well-Consolidated and Non-Flexible Behavioral State." In: *Scientific Reports* 9.1 (1 Dec. 30, 2019), p. 20259. ISSN: 2045-2322. DOI: 10.1038/s41598-019-56340-y. URL: https://www.nature.com/articles/s41598-019-56340-y (visited on 05/02/2023).

[6] Chloé Hegoburu et al. "The RUB Cage: Respiration-Ultrasonic Vocalizations-Behavior Acquisition Setup for Assessing Emotional Memory in Rats." In: *Frontiers in Behavioral Neuroscience* 5 (2011), p. 25. ISSN: 1662-5153. DOI: 10.3389/fnbeh.2011.00025. pmid: 21637320.

[7] Maxime Juventin et al. *Respiratory Rhythm Entrains Membrane Potential and Spiking of Non-Olfactory Neurons*. URL: https://hal.science/hal-03765341. preprint.

[8] Laura Lefèvre et al. "Significance of Sniffing Pattern during the Acquisition of an Olfactory Discrimination Task." In: *Behavioural Brain Research* 312 (Oct. 1, 2016), pp. 341–354. ISSN: 0166-4328. DOI: 10.1016/j.bbr.2016.06.039. URL: https://www.sciencedirect.com/science/article/pii/S0166432816303941 (visited on 05/02/2023).

[9] Felix Mölder et al. "Sustainable Data Analysis with Snakemake." In: 10:33 (Jan. 18, 2021). DOI: 10.12688/f1000research.29032.1. URL: https://f1000research.com/articles/10-33 (visited on 05/25/2023).

[10] Martin Vinck et al. "An Improved Index of Phase-Synchronization for Electrophysiological Data in the Presence of Volume-Conduction, Noise and Sample-Size Bias." In: *NeuroImage* 55.4 (Apr. 15, 2011), pp. 1548–1565. ISSN: 1053-8119. DOI: 10.1016/j.neuroimage.2011.01.055. URL: https://www.sciencedirect.com/science/article/pii/S1053811911000917 (visited on 06/16/2023).